Discrete Lange-Newell criterion for dissipative systems

Fabien II Ndzana,[1,*] Alidou Mohamadou,[1,2,3,†] and Timoleon Crépin Kofané[2,3,‡]
[1]*Department of Physics, Faculty of Science, Laboratory of Mechanics, University of Yaounde I, P.O. Box 812, Yaounde, Cameroon*
[2]*Department of Physics, Faculty of Science, Condensed Matter Laboratory, University of Douala, P.O. Box 24157, Douala, Cameroon*
[3]*The Abdus Salam, International Center For Theoretical Physics, P.O. Box 586, Strada Costiera, 11, I-34014 Trieste, Italy*
(Received 17 December 2008; published 29 May 2009)

We report on the derivation of the discrete complex Ginzburg-Landau equation with first- and second-neighbor couplings using a nonlinear electrical network. Furthermore, we discuss theoretically and numerically modulational instability of plane carrier waves launched through the line. It is pointed out that the underlying analysis not only spells out the discrete Lange-Newell criterion by the means of the linear stability analysis at which the modulational instability occurs for the generation of a train of ultrashort pulses, but also characterizes the long-time dynamical behavior of the system when the instability grows.

DOI: 10.1103/PhysRevE.79.056611 PACS number(s): 05.45.Yv, 42.25.Bs, 42.65.Tg, 84.40.Az

I. INTRODUCTION

Dissipative systems are common in nature. Strictly speaking, any other physical model is just an idealization. The so-called conservative or Hamiltonian systems provide convenient models for basic mathematical analysis of simple motion, but they fail to describe real dynamics in longer time scales. Observing nature, we can realize that "particles" are always submerged into dissipative media, which feed their continuous motion. Dissipative systems driven far from thermal equilibrium support solitonlike localized states. These structures are referred to as "dissipative solitons" and are sustained because of an interplay between dispersion, nonlinearity gain, and losses. One of the models of a dissipative system is based on the complex Ginzburg-Landau (CGL) equation [1] that has terms responsible for a variety of gain-loss mechanism. This equation is encountered in several diverse branches of physics, such as, for example, in superconductivity and superfluidity, nonequilibrium fluid dynamics and chemical systems, nonlinear optics, Bose-Einstein condensates, quantum field theories, and nonlinear electrical line [1–4]. The discrete CGL lattices are quite often used to describe a number of physical systems such as semiconductor laser in optics [5] as well as the formation of dissipative discrete solitons in laser arrays [6], Taylor and frustrated vortices in hydrodynamics [7].

Also, the behavior of nonlinear discrete system has received considerable attention. There are two main raisons for this interest: the development of experimental techniques making it possible to realize experiment in complicated periodic nonlinear structure and the potential for all-optical switching applications. The nonlinear electrical lines are good examples of such systems. They are very convenient tools for studying quantitatively the fascinating properties of wave propagation in nonlinear dispersive media [8,9]. In particular, they provide a useful way to check directly how the nonlinear excitations behave inside the nonlinear medium by means of probes related to an oscilloscope. The first studies of soliton on electrical lattices have been done by Hirota and Suzuki [8]. Qualitatively, the origin of soliton in nonlinear electrical line is explained by the balance between the effect of dispersion (due to the periodic location of capacitor in the nonlinear electrical lines) and nonlinearity (due to the voltage dependence of the capacitance). Let us also point out that, recently, nonlinear electrical lines have proven to be of great practical use in extremely wideband (frequencies from dc to 100 GHz) focusing and shaping of signals [10] which is usually a hard problem. Up to now, in the area of dissipative lattices, only the one-dimensional discrete CGL equation with first-neighbor couplings has been derived in any physical system.

In this work, we report the first derivation of the discrete CGL equation with first- and second-neighbor couplings in a real network: the nonlinear electrical line. A fundamental process that is possible in such an array system is that of discrete modulational instability (MI). Thereafter, the generalized discrete Lange-Newell criterion will be derived for dissipative systems. Our numerical observations were found to be in good agreement with theoretical predictions. The paper is organized as follows. In Sec. II, we derive through the nonlinear electrical line, the discrete complex Ginzburg-Landau (DCGL) equation with next-nearest-neighbor couplings. The generalized Lange-Newel criterion is also presented. Section III is used to verify our analytical findings and good agreement is obtained. Finally in Sec. IV we give a brief summary.

II. DCGL WITH NEXT-NEAREST-NEIGHBOR COUPLINGS IN NONLINEAR ELECTRICAL LATTICE

We consider a nonlinear electrical line which contains a finite number of cells as shown in Fig. 1. Each cell contains a linear inductor of inductance L_1 and L_3 in the series branch and a linear inductor of inductance L_2 in parallel with a nonlinear capacitor C. This capacitor consists of a reverse-biased diode with a differential capacitance function of the voltage V_n across the capacitor. The conductance g_1 describes the dissipation in the inductor L_1 while g_2 accounts for the dissipation of the inductor L_2 in addition to the loss of the

*ndzanafabienii@yahoo.com
†mohdoufr@yahoo.fr
‡tckofane@yahoo.com

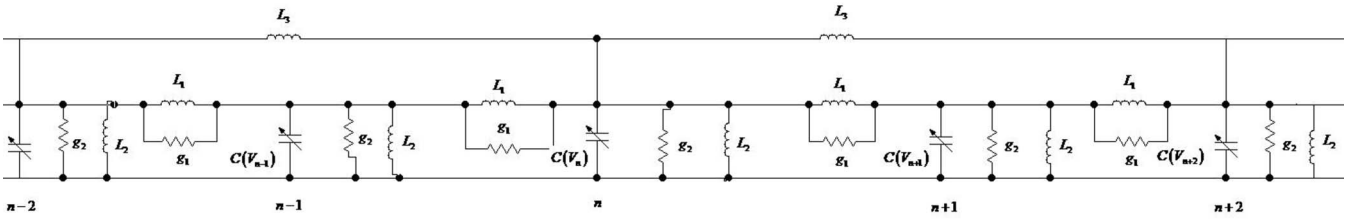

FIG. 1. Schematic representation of the nonlinear electrical line.

nonlinear capacitor $C(V_n)$. During computations, the following values of parameters are used: $L_1=L_3=280$ μH [10,11,13] and $L_2=2L_1=560$ μH. The nonlinearity is introduced in the line by a varicap diode for which the capacitance varies with the applied tension. Denoting by $Q_n(t)$ the nonlinear electrical charge of the nth cell and by $V_n(t)$ the corresponding voltage, we assume that the charge has a voltage dependence similar to the one of an electrical Toda lattice [12]: $Q_n=C_0A\ \ln(1+\frac{V_n(t)}{A})$. The subscript n designates the number of cells in the network. Coefficients A and C_0 are constants. Negative nonlinear resistances are made of operational amplifiers, transistors, or multipliers. They were introduced recently in nonlinear transmission lines for signal processing applications, particularly in noise removal on coherent information weakly varying in space [13] and on image and waves amplification [14]. The corresponding conductance is given by $g_2=\alpha-\beta V_n$.

We focus now on the nonlinear behavior of the lattice. From Kirchhoff's laws it is easy to show that the propagation of waves in the network is governed by the following equation:

$$
\begin{aligned}
&(A+V_n)\frac{d^2V_n}{dt^2}-\left(\frac{dV_n}{dt}\right)^2 \\
&\quad=\frac{\mu_0^2}{A}(A+V_n)^2(V_{n-1}-2V_n+V_{n+1})-\frac{\omega_0^2}{A}(A+V_n)^2V_n \\
&\quad+\frac{\Omega_0^2}{A}(A+V_n)^2(V_{n-2}-2V_n+V_{n+2}) \\
&\quad+2\sigma_1\frac{\mu_0}{A}\left(\frac{d(V_{n-1}-2V_n+V_{n+1})}{dt}\right)-2\sigma_2\frac{\mu_0}{A}(A+V_n)^2\frac{dV_n}{dt} \\
&\quad+2\beta'\frac{\mu_0}{A}(A+V_n)^2\frac{dV_n^2}{dt},
\end{aligned}
\tag{1}
$$

where $2\mu_0\sigma_1=\frac{g_1}{C_0}$, $2\mu_0\beta'=\frac{\beta}{C_0}$, $2\mu_0\sigma_2=\frac{\alpha}{C_0}$, $\omega_0^2=\frac{1}{L_2C_0}$, $\mu_0^2=\frac{1}{L_1C_0}$. The linear properties of the network can be studied by assuming a sinusoidal wave and, thus one obtains the following dispersion relation of the line plotted in Fig. 2:

$$
\omega_2^2=\omega_0^2+4\mu_0^2\sin^2\left(\frac{k}{2}\right)+4\Omega_0^2\sin^2(k). \tag{2}
$$

From Eq. (2), one can derive the following group velocity:

$$
V_g(k)=\frac{\mu_0^2\sin(k)+2\Omega_0^2\sin(2k).}{\sqrt{\omega_0^2+4\mu_0^2\sin^2\left(\frac{k}{2}\right)+4\Omega_0^2\sin^2(k)}}. \tag{3}
$$

This group velocity increases by including second-order couplings as one can see in Fig. 3. We restrict our study to slow temporal variations in the envelope. As we shall see, it provides a deep and useful insight into the full dissipative dynamics of the nonlinear electrical line and leads to pattern formation. For this purpose, we look for a solution of Eq. (1) in the form

$$
V_n=\varepsilon\psi_n(T)\exp(-i\omega t)+\varepsilon\psi_n^*(T)\exp(i\omega t), \tag{4}
$$

where ε is small parameter ($\varepsilon\ll 1$) and $T=\varepsilon^2t$. Inserting this relation in Eq. (1), we collect solutions of order $(\varepsilon,\exp(-i\omega t))$, order $(\varepsilon^2,1)$ which give a relation between the wave function at different site of the lattice. Thereafter, one write the relation at order $[\varepsilon^3,\exp(-i\omega t)]$, using the dispersion relation [Eq. (2)] and equations resulting from the above different order, one obtains the following equation:

$$
\begin{aligned}
&i\phi_{n\tau}+P_1(\phi_{n-1}-2\phi_n+\phi_{n+1})+P_2(\phi_{n-2}-2\phi_n+\phi_{n+2}) \\
&\quad+Q|\phi_n|^2\phi_n=i(\gamma_r+i\gamma_i)\phi_n,
\end{aligned}
\tag{5}
$$

where the complex coefficients of Eq. (4) are given by

$$
Q_r=\frac{3\omega^2}{A^2\mu_0^2},
$$

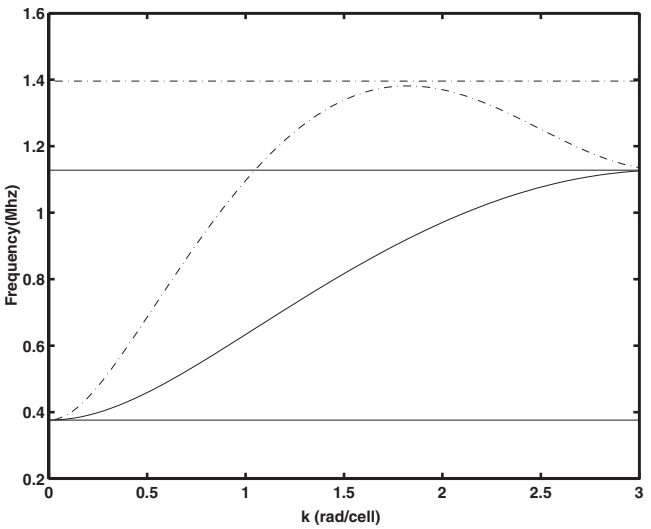

FIG. 2. Linear dispersion curve.

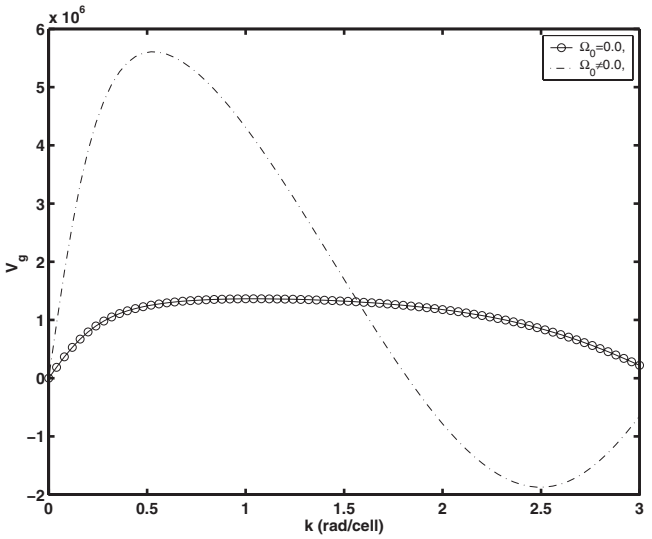

FIG. 3. Group velocity.

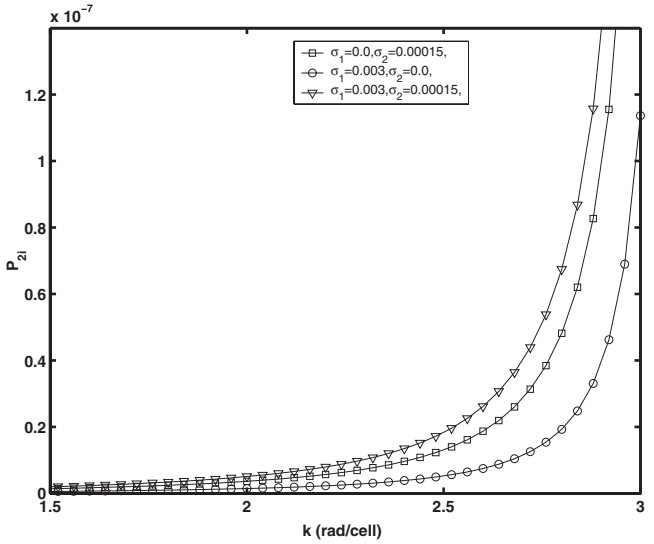

FIG. 4. Dependence of the second-neighbor coefficient P_{2i} with the wave number k.

$$Q_i = \frac{4\beta'\omega}{A\mu_0^2},$$

$$P_{1r} = 1,$$

$$P_{2r} = \frac{\Omega_0^2}{\mu_0^2},$$

$$P_{1i} = 2\frac{\omega}{\mu_0}\left[\frac{\sigma_1(\omega_0^2 + 2\mu_0^2 + 2\Omega_0^2 - \omega^2) - \mu_0^2(\sigma_2 + 2\sigma_1)}{\omega_0^2 + 2\mu_0^2 + 2\Omega_0^2 - \omega^2}\right],$$

$$P_{2i} = 2\frac{\omega}{\mu_0}\left[\frac{\Omega_0^2(\sigma_2 + 2\sigma_1)}{\omega_0^2 + 2\mu_0^2 + 2\Omega_0^2 - \omega^2}\right],$$

$$\gamma_i = 2(P_{1r} + P_{2r}),$$

$$\gamma_r = -2(P_{1i} + P_{2i}).$$

Figure 4 presents the dependence of the coefficient P_{2i} versus the wave number for different values of the parameter σ_i $(i=1,2)$. Equation (5) is the so-called discrete cubic CGL equation with first- and second-neighbor couplings. This equation has been phenomenologically proposed to describe frustrated states in a linear array of vortices [7]. Also, it reproduces reasonably well characteristics of the turbulent regime below the percolation threshold. Percolation has been found to be useful concept for the description of turbulence, and the results suggest that nonadiabatic effects, such as discrete nature of the system, play a role in the system. Let us point out that the first study of second-order coupling has been done by Efremidis *et al.* [15] through the study of discrete diffraction properties of nonlinear waveguide arrays. Later, a general model of a one-dimensional dynamical lattice combining the on-site discrete nonlinear Schrödinger equation nonlinearity and both the first couplings and second couplings linear couplings between lattice sites has been introduced [16]. This model has been considered to describe three types of fundamental solitons: site-centered and intersite-centered ones, and twisted localized modes.

MI has time-honored history in nonlinear wave equations. Their occurrence span areas ranging from fluid dynamics [17] (where they are usually referred to as the Benjamin-Feir instability) and nonlinear optics [18,19] to plasma physics [20]. While earlier manifestation of such instabilities was studied in continuum systems, in the last decade the role of the MI in the dynamics of discrete systems has emerged. In particular, the MI was analyzed in the context of the discrete nonlinear Schrödinger equation [21].

The fundamental idea of linear stability analysis is to perturb the initial solution slightly, and then study whether this small perturbation grows or decays with propagation. It should be emphasized that the linear stability analysis is valid as long as the perturbation amplitude remains small compared with the initial wave amplitude. So, to study the MI, we assume an initial wave. The stability properties of the initial wave can be determined by perturbing the initial wave,

$$\phi_n(\tau) = [\phi_0 + B_n(\tau)]\exp[i(kn - \omega\tau)], \tag{6}$$

where ϕ_0 is the initial complex constant amplitude, k and ω are, respectively, the wave number and the angular frequency of the carrier wave. The quantity $B_n(\tau)$ is the perturbation assumed to be small in comparison of ϕ_0. To further analyzed this problem, we write

$$B_n = b_1 \exp[i(Kn + \Omega\tau)] + b_2^* \exp[-i(Kn + \Omega^*\tau)], \tag{7}$$

where K and Ω are the wave number and the frequency of perturbation, respectively. While K is real, Ω may be complex. Parameters b_1 and b_2 are complex constants. With this relation of the perturbation, Eq. (7) leads to a linear homogenous system for b_1 and b_2. The condition for the nontrivial solution of this linear homogenous system gives a second-order equation for Ω,

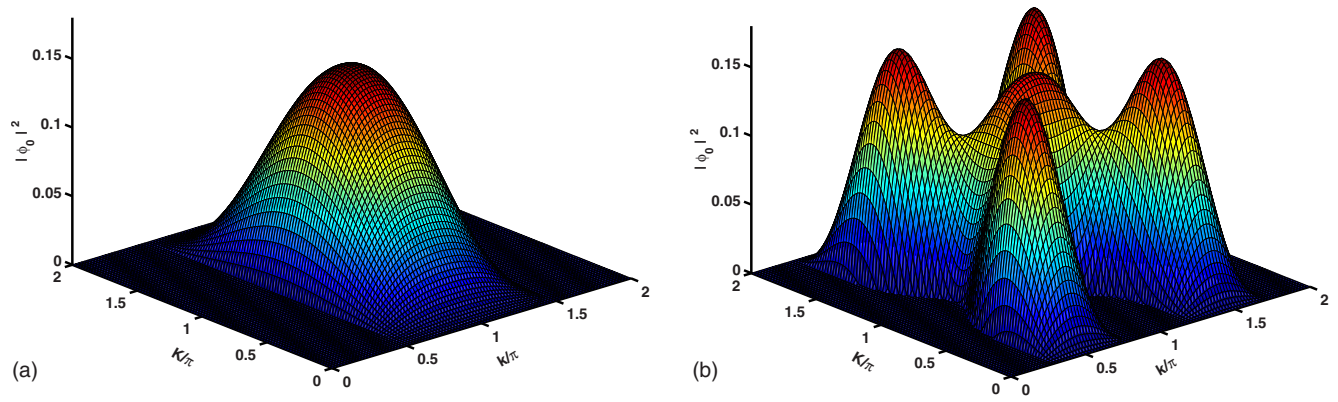

FIG. 5. (Color online) Threshold amplitude on the (K,k) plane: (a) without second-neighbor; (b) with the contribution of second neighbor.

$$[\Omega - \lambda_r - i\lambda_i]^2 = \xi_r + i\xi_i, \tag{8}$$

where λ_r, λ_i, ξ_r, and ξ_i are given in the Appendix. The frequency Ω can be written as

$$\Omega = \left[\lambda_r \pm \sqrt{\frac{(\xi_r + |\xi|)}{2}}\right] + i\left[\lambda_i \pm \sqrt{\frac{(-\xi_r + |\xi|)}{2}}\right]. \tag{9}$$

Substituting Eq. (9) into Eq. (7) helps in understanding the behavior of waves in the network. Indeed, this operation yields

$$B_n(\tau) = \left\{ b_1 \exp\left[i\left(Kn + \left(\lambda_r \pm \sqrt{\frac{(-\xi_r + |\xi|)}{2}} \right)\tau \right)\right] + b_2^* \exp\left[-i\left(Kn + \left(\lambda_r \pm \sqrt{\frac{(-\xi_r + |\xi|)}{2}} \right)\tau \right)\right]\right\} \times \exp\left\{ -\left[\lambda_i \pm \sqrt{\frac{(-\xi_r + |\xi|)}{2}} \right]\tau \right\}. \tag{10}$$

The amplitude $B_n(\tau)$ will be unbounded as $\tau \to +\infty$ if and only if: $\lambda_i \pm \sqrt{\frac{(-\xi_r+|\xi|)}{2}} < 0$, in order to get this relation, it is necessary that $\lambda_i < 0$. Because, $-\sqrt{\frac{(-\xi_r+|\xi|)}{2}} < 0$, the relation, $\lambda_i - \sqrt{\frac{(-\xi_r+|\xi|)}{2}} < 0$, holds and from this inequality we can easily derive the following inequality,

$$|\phi_0|^2 \leq |\phi_0|^2_{cr} = \left| \frac{4P_{2i}\sin^2(K)\cos(2k) + 4P_{1i}\sin^2(K/2)\cos(k)}{Q_i} \right|. \tag{11}$$

Relation (11) represents the threshold amplitude of wave through the system. As a first step, it is interesting to see how the threshold amplitude depends on the presence of first- and second-neighbor couplings. Thus, this threshold is depicted in Fig. 5. Figure 5(a) shows the threshold amplitude in the absence of second-neighbor couplings, while Fig. 5(b) shows the case where the second-neighbor couplings are taken into account. One can see that the competitive effects between first- and second-neighbor couplings lead to an explosion of the threshold in satellite sidebands.

Assume that the necessary condition $\lambda_i - \sqrt{\frac{(-\xi_r+|\xi|)}{2}} < 0$ is satisfied, then we can write the inequality $2\lambda_i^2 < -\xi_r$, that is

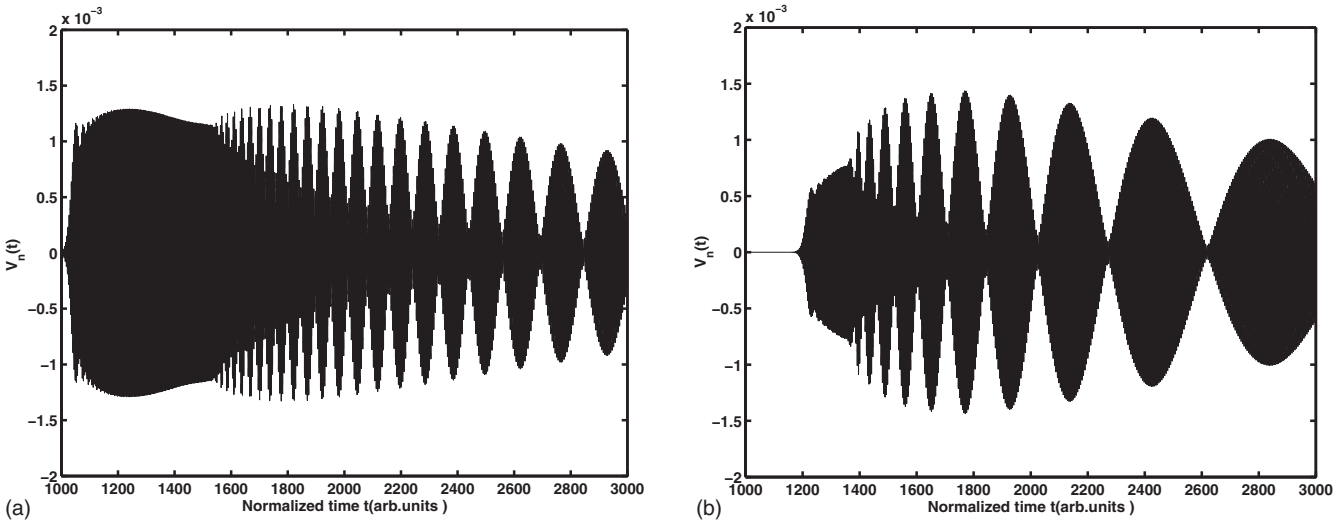

FIG. 6. Propagation of wave through the network in the absence of second-neighbor couplings: (a) Cell 800; (b) Cell 1000

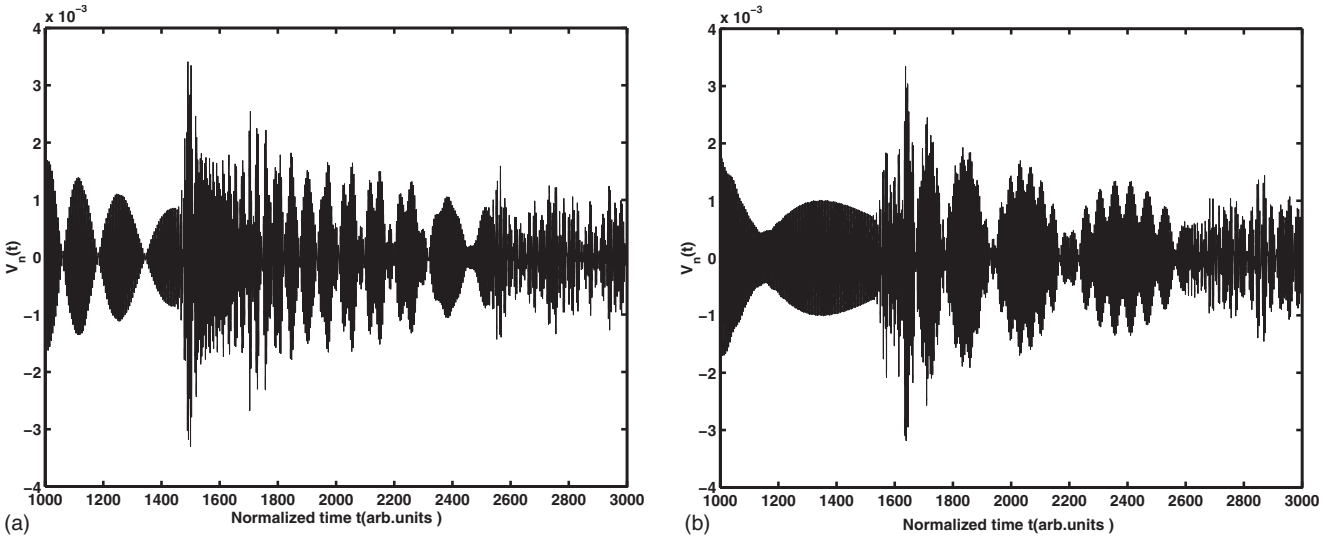

FIG. 7. Propagation of wave through the network in the presence of second-neighbor couplings: (a) Cell 800; (b) Cell 1000

$$(P_{1r}Q_r + P_{1i}Q_i)\sin^2(K/2)\cos(k) + 4(P_{2r}Q_r + P_{2i}Q_i)\cos^2(K/2)\cos(2k) + \frac{\Gamma}{8|\phi_0|^2\sin^2(K/2)} > \frac{2\lambda_i^2 + 16P_r^2\sin^4(K/2)\cos^2(k) + 16P_{2r}^2\sin^4(K)\cos^2(2k)}{8|\phi_0|^2\sin^2(K/2)} > 0, \quad (12)$$

where

$$\Gamma = 8\sin(K)\sin(k)[-P_{2i}P_{1i}\sin(2K)\sin(2k) + 4(P_{1i}P_{2i} + P_{1r}P_{2r})\sin^2(K)\cos(2k)]. \quad (13)$$

Relation (12) represents the MI criterion associated to the model understudy. This result is the discrete version of the well-known Lange and Newell criterion for discrete system. So, one can call this relation the generalized discrete Lange and Newell criterion.

In particular, when $P_{1i}=P_{2i}=P_{2r}=Q_i=\gamma_r=0$, Eq. (5) is reduced to the usual (nonintegrable) discrete nonlinear Schrödinger equation [21] and, one recovers results of Ref. [21], which in turn leads, in the continuum limit, to the well-known Benjamin-Feir instability [17]. In the long-wavelength limit, when $k \ll 1$ and $K \ll 1$: for $P_{2i}=P_{2r}=0$, the continuous analog of Eq. (5) is the continuous CGL equation [22]. In this case, relation (12) also fulfills the well-known Lange and Newell criterion for continuous lattices.

III. NUMERICAL ANALYSIS

To verify our analytical findings and to further explore MI, we use computer simulations. In particular, our results are based on the theory of linear stability analysis. However, we know that the linear stability analysis is limited because it can only predict the onset of instability and does not tell us anything about the long-time dynamical behavior of the system when the instability grows. When the perturbation amplitude grows large enough to be comparable to that of the initial wave, the numerical analysis must be adopted. To further confirm that our linear instability analysis given above can correctly describe the initial stage of instability in the nonlinear electrical lines, we exactly solve Eq. (1) by numerical fourth-order Runge-Kutta algorithm. A normalized integration time step $\Delta t=5\times10^{-3}$ is used for numerical simulations. Similarly, the number of cells N is chosen to be equal to 1500 and we have used periodic boundary conditions so that we do not encounter the wave reflection at the end of the line. At the input of the line, we apply a slowly modulated signal,

$$V(t) = V_0[1 + m_0\cos(2\pi f_m t)]\cos(2\pi f_p t), \quad (14)$$

where V_0 is the amplitude of the unperturbed plane wave, m_0 designates the modulation rate and f_m the frequency of modulation. As a specific example, we use the following value $V_0=0.80$ V, $f_p=1000$ KHz, $m_0=0.01$ and $f_m=12$ KHz. It is well known that a continuous wave or quasicontinuous radiation propagating in a nonlinear dispersive medium may suffer instability with respect to weak periodic modulations of the steady state and results in the breaking of a continuous wave into a train of ultrashort pulses. The above input signal voltage leads to a self-modulation of the wave as represented in Fig. 6 at different cells in the presence of dissipation term ($\sigma_1=0.003$ and $\sigma_2=0.00015$) with $\Omega_0=0$ i.e., in the absence of second neighbors. Figure 6(a) presents the time evolution of the voltage at cell 800, while Fig. 6(b) is depicted at cell 1000. In all these figures, one observes that the initial quasicontinuous is broken into a train of ultrashort pulses. The time evolution shape of the ultrashort pulses depends not only on parameters of the system but also on the different cells. The generation of high-repetition-rate pulse trains resulting from MI has been first suggested by Hasegawa and Brinkman [23] and it was later experimentally verified by Tai *et al.* [23]. Each element of the wave train which propagate in Fig. 6 has the shape of solitonlike object. One of the main properties of solitons, making them to be of special interest for physical applica-

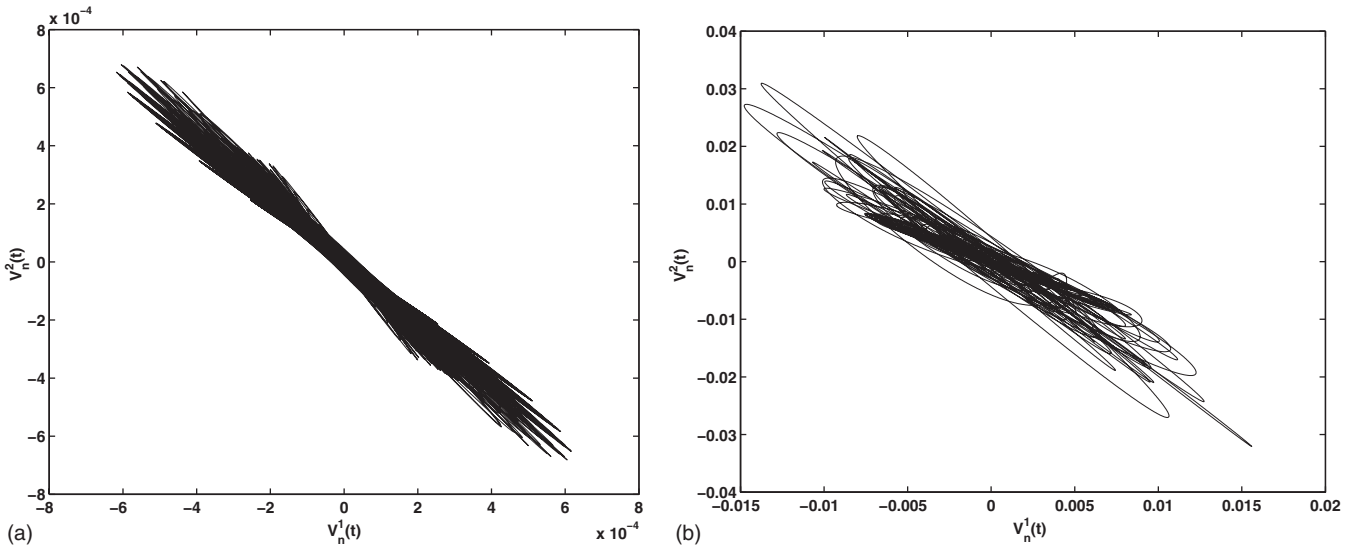

FIG. 8. Phase portrait at Cell 1000: (a) in absence of second-neighbor couplings; (b) in presence of second-neighbor couplings

tions, is preserving their localized shapes during evolution and mutual interactions. Due to this robustness, solitons can be regarded as quasiparticles and systems possessing large number of such excitations can be described in terms of the distribution function governed by the kinetic equation. The propagation presented in Fig. 6 is similar to the quantum evolution of Bose-Einstein condensate atom [24]. While in the presence of second neighbors, one obtains the phenomenon depicted in Fig. 7. Even in this case, the initial wave breaks into a pulse train. But due to the competitive effect between first- and second-neighbor couplings, the magnitude of voltage seems to increase slowly. What is also known at this level is the fact that the modulated waves seem to travel with chaoticlike behavior through the line.

Coherent structures and chaotic states are well known as two distinct states of nonlinear dissipative wave systems. However, these states sometimes occur and propagate together in some systems. Figure 8 depicts the incoherent evolution of modulated plane waves through the line. This incoherent evolution of modulated plane waves can also be evidenced from the nonreproducibility of experiments devoted to their propagation in the nonlinear medium, as observed by Ablowitz *et al.* [25] in the context of fluid dynamics, that is, considering modulated periodic Stokes waves in deep water. For two different experiments with initial identical signals generated by the wave maker, the resulting temporal evolutions of the surface displacement at a given position in the tank are graphed against each other to produce a "phase plane" plot indicating the level of reproducibility. In the phase plane plots, the evolution of the voltage $V_n^1(t)$ is graphed against the evolution of the voltage $V_n^2(t)$, $V_n^1(t)$, and $V_n^2(t)$ being the temporal voltages measured at the same cell n, and obtained using the same input signal $V(t)$ for the different experiments. Figure 8(a) presents the dynamics of the line in the absence of second neighbors. The graph traduces the dynamics of nonlinear modulated waves behaving an apparently chaoticlike state, at cells 1000. But when we take into account second neighbors, the system seems to become more chaotic as depicted in Fig. 8(b). One can conclude that the presence of second neighbors through the line seems to lead the system toward a chaoticlike behavior.

IV. CONCLUSION

In summary, we have reported the first derivation of the discrete complex Ginzburg-Landau equation with first- and second-neighbor couplings in a discrete nonlinear electrical lattice. The generalized discrete Lange-Newell criterion has been presented. As the quintic nonlinearity, we have demonstrated that the second-neighbor couplings can be used to control the magnitude of waves, and also can lead the system in a chaoticlike behavior. Results which have been presented in this work can be also appropriate in the context of multidisciplinary subjects.

APPENDIX

Coefficients of the linear homogenous system (8),

$$a = -4P_1 \sin^2\frac{K}{2}\cos(k) + 2P_1\sin(K)\sin(k) - 4P_2 \sin^2(K)\cos(2k) + 2P_2 \sin(2K)\sin(2k) + Q|\phi_0|^2,$$

$$b = -4P_1^* \sin^2\frac{K}{2}\cos(k) + 2P_1^* \sin(K)\sin(k) - 4P_2^* \sin^2(K)\cos(2k) + 2P_2^* \sin(2K)\sin(2k) + Q^*|\phi_0|^2,$$

$$\lambda_r = -2P_{1r} \sin(K)\sin(k) - 2P_{2r} \sin(2K)\sin(2k),$$

$$\lambda_i = Q_i|\phi_0|^2 - 4P_{1i} \sin^2\frac{K}{2}\cos(k) - 4P_{2i} \sin^2(K)\cos(2k),$$

$$\xi_r = \mathrm{Re}\left[\frac{1}{4}(b-a)^2 + ab - (Q_r^2 + Q_i^2)|\phi_0|^4\right],$$

$$\xi_i = \mathrm{Im}\left[\frac{1}{4}(b-a)^2 + ab - (Q_r^2 + Q_i^2)|\phi_0|^4\right].$$

[1] I. S. Aranson and L. Kramer, Rev. Mod. Phys. **74**, 99 (2002); M. C. Cross and P. C. Hohemberg, *ibid.* **65**, 851 (1993).
[2] Y. Kuramoto, *Chemical Oscillations, Waves and Turbulence* (Springer, Berlin, 1984).
[3] N. N. Akhmediev and A. Ankiewicz, *Solitons, Nonlinear Pulses and Beams* (Chapman and Hall, London, 1997).
[4] F. II Ndzana, A. Mohamadou and T. C. Kofane, J. Phys. D **40**, 3254 (2007).
[5] S. S. Wang and H. G. Winful, Appl. Phys. Lett. **52**, 1774 (1988).
[6] N. K. Efremidis and D. N. Christodoulides, Phys. Rev. E **67**, 026606 (2003).
[7] H. Willaime, O. Cardoso, and P. Tabeling, Phys. Rev. Lett. **67**, 3247 (1991); A. Mohamadou, A. K. Jiotsa, and T. C. Kofane, Phys. Rev. E **72**, 036220 (2005).
[8] R. Hirota and K. Suzuki, Proc. IEEE **61**, 1483 (1973); K. Lonngren, in *Solitons in Action*, edited by K. Lonngren and A. Scott (Academic, New York, 1978), pp. 127–152.
[9] M. Remoissenet, *Waves Call Solitons* 3rd ed. (Springer, Berlin, 1999); A. C. Scott, *Active and Nonlinear Wave Propagation in Electronics* (Wiley-Interscience, New York, 1970).
[10] E. Afshari and A. Hajimiri, IEEE J. Solid-State Circuits **40**, 744 (2005).
[11] D. Yemélé, P. Talla, and T. C. Kofané, J. Phys. D **36**, 1429 (2003).
[12] M. Toda, *Theory of Nonlinear Lattice* (Springer, Berlin, 1978).
[13] P. Marquie, S. Binczak, J. C. Comte, B. Michaux, and J. M. Bilbault, Phys. Rev. E **57**, 6075 (1998).
[14] J. S. Comte, P. Marquie, J. M. Bilbault, and S. Binczak, Ann. Telecommun. **53**, 483 (1998); H. K. Nguena, S. Noubissie, and P. Woafo, J. Phys. Soc. Jpn. **73**, 1147 (2004).
[15] N. K. Efremidis and D. N. Christodoulides, Phys. Rev. E **65**, 056607 (2002).
[16] P. G. Kevrekidis, B. A. Malomed, A. Saxena, A. R. Bishop, and D. J. Frantzeskakis, Physica D **183**, 87 (2003).
[17] T. B. Benjamin and J. E. Feir, J. Fluid Mech. **27**, 417 (1967).
[18] G. P. Agrawal, *Nonlinear Fiber Optics* (Academic Press, San Diego, CA, 1995).
[19] M. Soljacic, M. Segev, T. Coskun, D. N. Christodoulides, and A. Vishwanath, Phys. Rev. Lett. **84**, 467 (2000); J. Meier, G. I. Stegeman, D. N. Christodoulides, Y. Silberberg, R. Morandotti, H. Yang, G. Salamo, M. Sorel, and J. S. Aitchison, *ibid.* **92**, 163902 (2003).
[20] T. Taniuti and H. Washimi, Phys. Rev. Lett. **21**, 209 (1968).
[21] Y. S. Kivshar and M. Peyrard, Phys. Rev. A **46**, 3198 (1992); D. Hennig, Eur. Phys. J. B **20**, 419 (2001).
[22] C. G. Lange and A. C. Newell, SIAM J. Appl. Math. **27**, 441 (1974); A. K. Jiotsa and T. C. Kofane, J. Phys. Soc. Jpn. **72**, 1800 (2003).
[23] A. Hasegawa and W. F. Brinkman, IEEE J. Quantum Electron. **16**, 694 (1980); K. Tai, A. Hasegawa, and A. Tomita, Phys. Rev. Lett. **56**, 135 (1986).
[24] V. S. Shchesnovich and V. V. Konotop, Phys. Rev. A **75**, 063628 (2007).
[25] M. J. Ablowitz, J. Hammack, D. Henderson, and C. M. Schober, Physica D **416**, 152 (2001).